GEOLOGIJA 68/201-219, Ljubljana 2025

https://doi.org/10.5474/geologija.2025.008

Article

Carbon cycling dynamics in the headwater Radovna stream recharged by Lipnik springs, a carbonate catchment in the Julian Alps, Slovenia, based on stable isotope analysis

Dinamika kroženja ogljika v zgornjem toku potoka Radovna, ki ga napajajo izviri Lipnik, znotraj karbonatnega zaledja v Julijskih Alpah (Slovenija), na podlagi analize stabilnih izotopov

Tjaša KANDUČ[1]*, Timotej VERBOVŠEK[2] & Nataša MORI[3]

[1]Department of Environmental Sciences, Jožef Stefan Institute, Jamova cesta 39, SI-1000 Ljubljana, Slovenia; *corresponding author: tjasa.kanduc@ijs.si
[2]Department of Geology, Faculty of Natural Sciences and Engineering, University of Ljubljana, Aškerčeva 12, SI-1000 Ljubljana, Slovenia; e-mail: timotej.verbovsek@ntf.uni-lj.si
[3]Department of Organisms and Ecosystem Reserach, National Institute of Biology, Večna pot 121, 1000, Ljubljana, Slovenia; e-mail: natasa.mori@nib.si

Prejeto / Received 8. 4. 2025; Sprejeto / Accepted 21. 7. 2025; Objavljeno na spletu / Published online 10. 12. 2025

Key words: total alkalinity, stable isotopes, carbon, pCO_2, headwater stream, Julian Alps
Ključne besede: totalna alkalnost, stabilni izotopi, ogljik, pCO_2, zgornji tok porečja, Julijske Alpe

Abstract

Carbon cycling was investigated monthly (July, August, September, October, November, March and May) from July 2023 to May 2024 in the Radovna stream originating from the permanent Lipnik spring in the Julian Alps, Slovenia using isotopic composition of carbon in dissolved inorganic carbon ($\delta^{13}C_{DIC}$) and particulate organic carbon ($\delta^{13}C_{POC}$). The investigated catchment is composed of massive coarse - crystal dolomite and limestone. Total alkalinity ranged from 2.2 to 2.7 mM and is characteristic for carbonate pristine environments. In-situ parameters e.g. dissolved oxygen ranged from 11.0 to 12.0 mg/L, pH from 7.9 to 8.1 and specific electrical conductivity from 275 to 318 μS/cm, respectively. The values of dissolved oxygen reflect that the water system is well oxygenated. CO_2 presented a source of carbon to the atmosphere during all investigated months. Oversaturation with CO_2 is 1.01 to 4.1 times of atmospheric value. $\delta^{13}C_{DIC}$ ranged from -11.8 to -9.7 ‰. This indicates that dissolved inorganic carbon under different discharge conditions mainly originates from the dissolution of carbonates (from 50.3 % to 57.3 %), followed by the degradation of organic matter (from 42.8 % to 49.7 %). Equilibration with atmospheric CO_2 has a negligible impact, ranging from 0.01 % to 0.11 %. $\delta^{13}C_{POC}$ in river water indicate sources such as plant debris, with $\delta^{13}C_{POC}$ of -29.4 ‰, and highly degraded soil organic matter, with $\delta^{13}C_{POC}$ of -24.9 ‰. The $\delta^{13}C_{DIC}$ and $\delta^{13}C_{POC}$ values are typical for a forest stream flowing over a limestone substrate. Strong statistical negative significant correlation was obtained between electrical conductivity and water temperature, mass of total suspended solids (m_{TSS}) and pH.

Izvleček

Ogljikov cikel smo preučevali mesečno (julij, avgust, september, oktober, november, marec, maj) od julija 2023 do maja 2024 v potoku Radovne, ki izvira iz stalnega izvira Lipnik v Julijskih Alpah, Slovenija, z uporabo izotopske sestave ogljika v raztopljenem anorganskem ogljiku ($\delta^{13}C_{DIC}$) in partikulatnem organskem ogljiku ($\delta^{13}C_{POC}$). Raziskano porečje je sestavljeno iz masivnega grobo-kristalnega dolomita in apnenca. Totalna alkalnost se je spreminjala od 2,2 do 2,7 mM in je značilna za karbonatna naravna okolja. In-situ parametri kot je raztopljen kisik so se spreminjali od 11,0 do 12,0 mg/L, pH od 7,9 do 8,1 mg/L, specifična elektroprevodnost pa od 275 do 318 μS/cm. Vrednosti raztopljenega kisika odražajo, da je vodni sistem dobro prezračen s kisikom. CO_2 predstavlja sproščanje ogljika v atmosfero iz potoka v vseh preiskanih mesecih. Prenasičenost s CO_2 je 1,01 do 4,1 krat večja od atmosferske vrednosti. $\delta^{13}C_{DIC}$ se je spreminjala od -11,8 ‰ do -9,7 ‰. To kaže, da raztopljeni anorganski ogljik pri različnih pretokih vode večinoma izvira iz raztapljanja karbonatov (od 50,3 % do 57,3 %), sledi pa razgradnja organske snovi (42,8 % do 49,7 %). Uravnoteženje z atmosferskim CO_2 ima zanemarljiv vpliv, v razponu od 0,01 % do 0,11 %. Partikulatni organski material (POC) izvira iz površinskega in podzemnega toka. $\delta^{13}C_{POC}$ v odvzeti vodi je odražal vir iz rastlinskih ostankov z $\delta^{13}C_{POC}$ -29,4 ‰ in razgrajenega preperinskega organskega materiala z $\delta^{13}C_{POC}$ -24,9 ‰. Vrednosti $\delta^{13}C_{DIC}$ in $\delta^{13}C_{POC}$ so tipične za gozdni potok, ki teče po apnenčasti podlagi. Močna, statistično značilna negativna korelacija je bila ugotovljena med elektroprevodnostjo in temperaturo vode, maso celotne suspendirane snovi (m_{TSS}) in pH.

Introduction

Rivers play a pivotal role in the global carbon cycle, acting as conduits that transport carbon between terrestrial, aquatic, and atmospheric systems. They facilitate the movement of dissolved inorganic carbon (DIC), dissolved organic carbon (DOC), and particulate organic carbon (POC), significantly influencing both local and global carbon dynamics (Battin et al., 2008). During high-flow events, rivers can export substantial amounts of DOC and POC through overland runoff, introducing plant-derived organic matter into aquatic environments. Moreover, rivers often serve as sources of carbon dioxide (CO_2) to the atmosphere (Raymond et al., 2013), with concentrations frequently surpassing ambient levels, underscoring their role as net CO_2 sources. Headwater streams (Richardson, 2019) directly reflect carbon input from soils and groundwaters and are important due to their large proportion in global river networks, representing more than 96 % of the total number of streams. As a result, they contribute significant amounts of CO_2 to the atmosphere, accounting for approximately 36 % (i.e., 0.93 Pg C yr−1) of total CO_2 outgassing from rivers and streams globally (Marx et al., 2017). The analysis by Marx et al., (2017) indicated that the global river average pCO_2 of 3100 ppm is more often exceeded by contributions from small streams when compared to rivers with larger catchments (> 500 km^2).

Stable isotopes, such as carbon isotopes (^{13}C and ^{12}C) in dissolved inorganic carbon (DIC), are particularly useful for tracing sources of carbon, understanding processes like photosynthesis, respiration, dissolution of carbonates/precipitation of carbonates within river systems (Kendall & McDonell, 1998; Lyons et al., 2013). Isotopic equilibrium between river water and the atmosphere has been demonstrated to be an exception in most cases (Gammons et al., 2011). Landscape, climate, catchment lithology, and vegetation type influence $\delta^{13}C_{DIC}$ values. In highly turbulent river systems, such as those with a torrential character or those exhibiting Alpine or Alpine – Dinaric flow regimes, photosynthesis can be neglected (Kanduč et al., 2007a). The $\delta^{13}C_{DIC}$ value is determined either by the fractionation that occurs during carbon transformation or by the mixing of carbon from different sources (Atekwana & Krishnamurthy, 1998; Doctor et al., 2008; Karlović et al., 2022; Knoll et al., 2024; Evans et al., 2024). The isotopic composition of particulate organic carbon ($\delta^{13}C_{POC}$) is related to its origin in the terrestrial environment, leaching from the terrestrial sources and in stream processes (Kanduč et al., 2007b; Waldron et al., 2018; Utsumi et al., 2025).

The main objective was to determine CO_2 saturation, and identify biogeochemical processes through carbon mass balance calculations, including organic matter degradation, carbonate dissolution and equilibration with atmospheric CO_2 using $\delta^{13}C_{DIC}$ in a small stream of the Radovna River in the Julian Alps, recharged by the permanent Lipnik Spring (Mori et al., 2015). Additionally, we investigated the origin of carbon in particulate organic carbon (POC) using $\delta^{13}C_{POC}$. The study provides important insights into the poorly understood role of headwater streams (Richardson, 2019) in global carbon dynamics.

Catchment characteristics of the studied headwater stream

The Lipnik spring system lies in the Julian Alps of northwestern Slovenia, at the foot of the Pokljuka plateau (Fig. 1). It consists of two intermittent springs and one permanent spring, with discharge elevations ranging from 665 to 692 m a.s.l. These sources give rise to a short stream that feeds into the Radovna River, which belongs to the upper Sava River catchment. Figure 1 illustrates the investigated small carbonate stream, a tributary of the Radovna River, originating from the permanent Lipnik spring. Located near the glacial valley of Krnica in Julian Alps, the Lipnik spring is a part of the Radovna–Mežakla aquifer system within the broader Sava River Basin. Tectonically, it belongs to the Julian Alps thrust, with the Mesozoic layers of the Kranjska Gora thrust to the north, and separated from the southern Karavanke mountain range and Košuta thrust by the Sava Fault (Fig. 1). The region features sedimentary layers with ages from the Lower Triassic to the Cretaceous, predominantly Upper Triassic carbonates. The catchment area (Fig. 1) comprises various geological formations. These include massive coarse-crystalline dolomite and limestone of Rhaetian and Cordevolian age, (number 84 on the map), platy micritic limestone with chert nodules from the Pokljuka Formation (number 87) and Middle Triassic (Anisian) dolomites (number 91). Additionally, there are Middle Triassic (Ladinian) clastic rocks and tuffs (number 90). Some parts of the massive and bedded Dachstein limestones transition into Main dolomites (number 76). The floor of the Radovna valley is covered with Quaternary fluvial deposits (number 12) and sections of unconsolidated moraine (number 14) are present (Fig. 1).

Hydrogeologically, the catchment is characterized by extensive, moderately to highly productive karst fracture aquifers, with smaller, localized

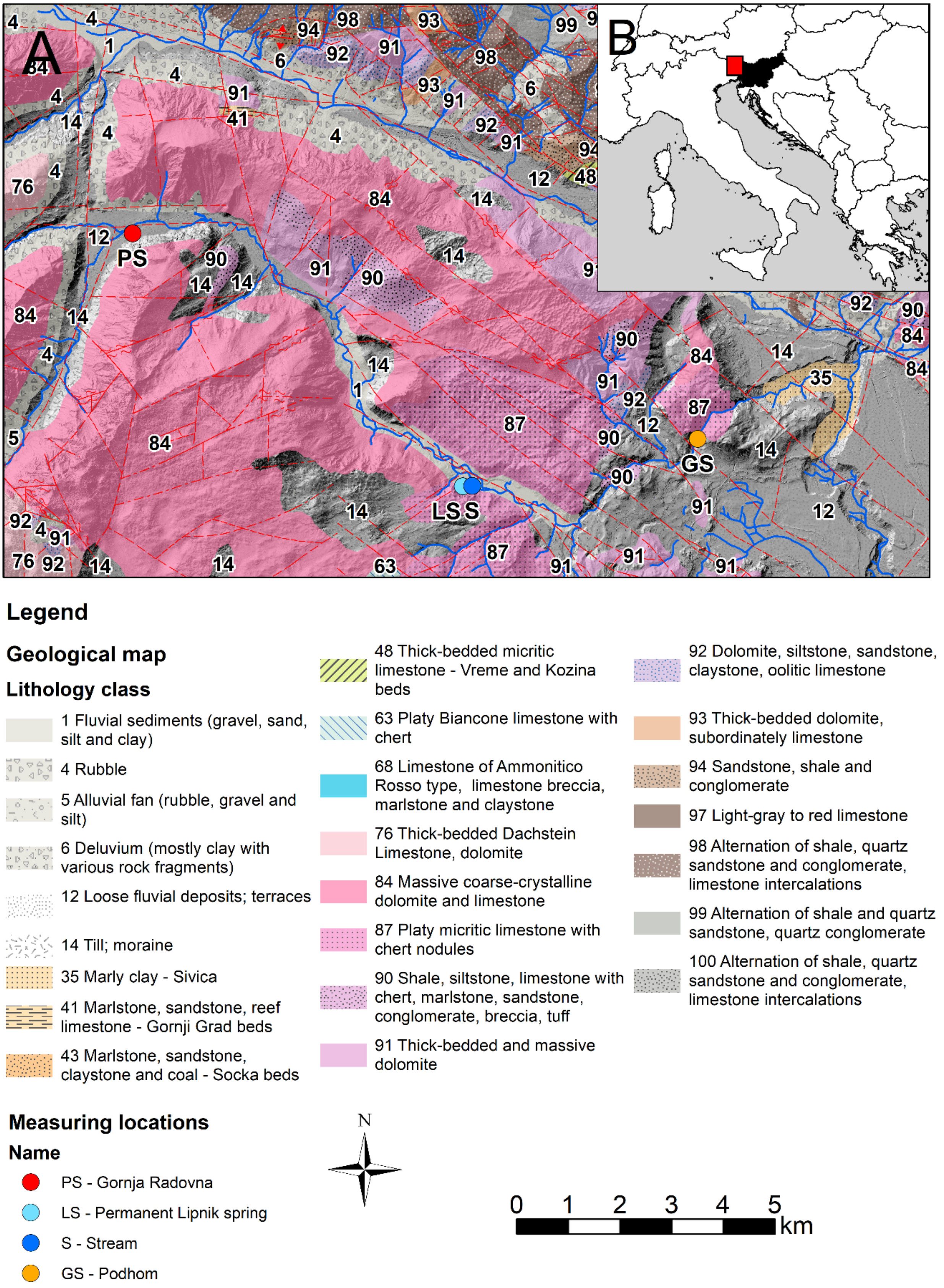

Fig. 1. A. Geological map with sampling location (S - stream recharged from permanent Lipnik spring, LS – Lipnik spring, PS – precipitation station Zgornja Radovna, GS – gauging station Podhom). B. Position of research catchment area (red square) in the broader region (Slovenia is filled with black color). Geological map is in the original scale of 1:250,000 (Buser & Komac, 2002).

groundwater sources in some areas. Hydrological data from Environment Agency of the Republic of Slovenia indicate a hydrological station on the Radovna River upstream of the Lipnik spring (1953-1972) and another downstream (1957–1966), with a significant difference of approximately 2 m^3/s between their average flows, which exceeds the expected discharge of the Lipnik spring. No other significant groundwater withdrawals occur within the catchment area (Internet 1). The investigated stream is fed by the permanent Lipnik spring (Fig. 1) through groundwater recharge, subsurface flow, and surface flow.

Numerous studies have previously examined both the permanent Lipnik spring (LS, Fig. 1) and the two temporary spring outlets of the Lipnik spring in the context of water geochemistry and aquatic fauna research (Kanduč et al., 2012; Mori & Brancelj, 2013; Mori et al., 2015; Opalički, 2015; Serianz et al., 2020). Investigation of δ^{18}O and ^{3}H tracers in Lipnik springs recharging investigated headwater stream indicated that springs are recharged from precipitation. The value of δ^{18}O ranged from -10.7 to -8.1 ‰ Main conclusions considering δ^{18}O and ^{3}H were that spring water did not differ between investigated springs. δ^{18}O of the spring water was lowest during spring due to melting of snow. Concentrations of tritium ranged from 5.5 to 6.9 TU for perennial spring and 4.0 to 7.5 TU for the temporary spring, which also indicated that spring water originated from precipitation (Mori et al., 2015). From the decay of tritium, the age of the spring water was estimated to be around 3.8 years (Kanduč et al., 2012) indicating a highly permeable aquifer with fast flowing water, which is typical of karst-fissured aquifers.

Methods

Sampling

Sampling was performed during different sampling seasons e.g. three times in summer (20/07/2023, 31/08/2023, 29/09/2023), autumn (24/10/2023, 29/11/2023), winter (18/03/2024) and spring (13/05/2024). Monthly sampling throughout the year is presented in Figure 2. The distance from the Lipnik spring to the sampling point is 160 m (Fig. 1), and the width of the stream at the sampling point (Fig. 2) is 4 m. Sampling was performed in the middle of the stream (Fig. 2). Associated precipitation and discharge data are provided in Table 1.

Fig. 2. Sampling of the stream recharging from the permanent Lipnik spring in different sampling months in August 2023 (photo by Nataša Mori).

Temperature (T), electrical conductivity, dissolved oxygen (DO) and pH of stream water were measured *in-situ* using a digital multiparameter portable meter (WTW, MultiLine® 3630 IDS). The measurement errors are as follows: for temperature ±0.1 °C, for pH ±0.004 units, and for dissolved oxygen (DO) ± 0.5 %. Samples for total alkalinity were filtered through a 0.45 µm VPDF filter and stored in 30 mL High Density Polyethylene (HDPE) bottles. Samples for $\delta^{13}C_{POC}$ analyses were collected in 5 L Low Density Polyethylene (LDPE) bottles, while samples for $\delta^{13}C_{DIC}$ analyses were filtered through 0.45 µm VPDF filter and stored in 12 mL glass serum bottles filled with no headspace to prevent gas exchange. Total alkalinity and $\delta^{13}C_{DIC}$ were analysed within 24 hours of sample collection.

Total alkalinity and isotopic analyses of carbon

The total alkalinity was measured using Gran titration, as described in detail by Zuliani et al. (2020). The stable isotope composition of dissolved inorganic carbon ($\delta^{13}C_{DIC}$) was determined using a Europa Scientific 20–20 continuous flow isotope ratio mass spectrometer (IRMS) with an ANCA–TG preparation module. The method is fully described in Zuliani et al. (2020). Filters used for determination of total suspended solids (m_{TSS}) mass and for $\delta^{13}C_{POC}$ analysis were preweighed. Five liters of stream water were filtered through a

Whatman GF/F glass fiber filter (0.7 µm pore size). The filters, coated with suspended matter, were dried at 60 °C and reweighed to calculate the total suspended solids (TSS) by comparing the pre- and post-filtration weights. After weighing, the filters were treated with 3 M HCl to remove carbonate material, dried again at 60 °C in a Memmert UN 55 oven and stored until analysis. Approximately 1 mg of particulate matter was scraped from the filters for $\delta^{13}C_{POC}$ analysis (Kanduč et al., 2012).

To calibrate the $\delta^{13}C_{POC}$ measurements, we used 0.05 mg of the IAEA CH-3 (-24.72‰±0.04) and IAEA CH-7 (-32.15 ‰±0.05) reference materials, along with a weighed sample of commercially available table sugar ($\delta^{13}C$ = -27.1‰±0.2) used as a working standard. The stable isotope composition of particulate organic carbon ($\delta^{13}C_{POC}$) was measured using a Europa Scientific 20-20 continuous flow isotope ratio mass spectrometer (IRMS) equipped with an ANCA–SL preparation module. The weighing of certified materials was performed using a Mettler AE240 scale.

A mass balance calculation for three months representing low, high, and intermediate discharge conditions (July 2023, October 2023, and May 2024) was performed to evaluate in-stream biogeochemical processes, including equilibration with atmospheric CO₂, degradation of organic matter, and dissolution of carbonates, using equations (1)–(4) described below.

The mass flux (F_{ex}) between the stream and the atmosphere can be calculated using the following equation (Broecker, 1974):

$$F_{ex} = D \cdot ([CO_2]_{eq} - [CO_2])/z \qquad (1)$$

Where:

D - represents the diffusion coefficient of CO_2 in water, with values of 1.26 10^{-5} cm^2 /s at 10 °C and 1.67 10^{-5} cm^2 /s at 20 °C (Jähne et al., 1987).

$[CO_2]_{eq}$ and $[CO_2]$ indicate concentrations of dissolved CO_2 at equilibrium with the atmosphere and the sampled water [mol·cm^{-3}], respectively.

z – empirical thickness of the water surface layer [cm]; this boundary layer is a thin film located at the interface between air and water, and its thickness varies depending on wind speed (Broecker et al., 1978) and water turbulence (Holley, 1977).

D/z represents thin gas transfer velocity, reflecting the height of the water column that equilibrates with atmospheric CO_2 over time. Based on an average wind speed of 4 m/s characteristic for Sava River watershed in Slovenia, D/z is 8 cm/h for calm waters, 18 cm/h and 115 cm/h very turbulent conditions.

Mass balance concentrations of dissolved inorganic carbon (DIC) in stream:

$$F_s = \pm F_{ex} + F_{org} + F_{carb.} \qquad (2)$$

Where:

$F = Q \cdot [DIC]$ (mol/s)

F_s (mol/s) – mass flow of dissolved inorganic carbon at stream sampling point

Q (m^3/s) – measured discharge at gauging station Podhom; the flow rate was taken from the nearest gauging station (Podhom, Fig. 1), which is not active within in stream itself. In the mass balance calculation, we consider the general hydrological conditions in the catchment area and calculate the individual contributions of biogeochemical processes in the mass balance. The stream sampling point has similar hydrographic characteristics as nearest gauging station.

[DIC] (mmol/L) – measured total alkalinity in stream samples

F_{ex} (mol/s) – the mass flux of dissolved inorganic carbon between the stream and the atmosphere calculated according to equation (1)

F_{org} (mol/s) – the mass flux of dissolved inorganic carbon due to degradation of organic matter

F_{carb} (mol/s) – the mass flux of dissolved inorganic carbon due to dissolution of carbonates

$F_{org.}$ and $F_{carb.}$ are unknowns in equation (2)

Isotopic mass balance, which includes mass flow and isotopic composition of individual biogeochemical processes (ex – equilibration with atmospheric CO_2, org - degradation of organic matter and carb - dissolution of carbonates), influencing $\delta^{13}C_{DIC}$ is expressed as follows:

$$F_s \cdot \delta^{13}C_s = \pm F_{ex} \cdot \delta^{13}C_{ex} + F_{org} \cdot \delta^{13}C_{org\cdot} + F_{carb} \cdot \delta^{13}C_{carb} \qquad (3)$$

$\delta^{13}C_s$ – isotopic composition of dissolved inorganic carbon in stream

$\delta^{13}C_{ex.}$ – isotopic composition of dissolved inorganic carbon if solely equilibration of CO_2 would influence DIC values, calculated according to eq. (4)

$\delta^{13}C_{org.}$.- average isotopic composition of carbon in particulate organic matter in stream with value of -27.1‰

$\delta^{13}C_{carb.}$ – average isotopic composition of carbon in carbonates composing the stream catchment with value of 3.3 ‰ (Kanduč et al., 2012)

Isotopic composition of DIC due to equilibration with atmospheric CO_2 (Levin et al., 1987)

$$\delta^{13}C_{DIC} = -(0.141 \cdot T) + 10.78 + (-7.8) \qquad (4)$$

$\delta^{13}C_{DIC}$ –isotopic composition of DIC in water that forms due to equilibrium with atmospheric CO_2; the isotopic composition of atmospheric CO_2 is -7.8 ‰ (Levin et al., 1987), T – water temperature [°C]

PHREEQC for Windows software (Parkhurst & Appelo, 1999) was used to calculate partial pressure of CO_2 (pCO_2). Following parameters of the water were used as input parameters: temperature (T), pH and total alkalinity (TA).

Spearman correlations (Table SM1) between measured quantities at $p<0.050$ were performed with a program Statistica 14.0.0.15, while scatterplots were performed with Excel version 2016 and Python program.

GIS Map Preparation

Visual presentation and distance measurements were performed in ESRI ArcMap 10.5.1 software. We used a geological map at a scale of 1:250,000 (Buser & Komac, 2002). Only the geological units, outcropping in the map extent, are presented on the map. Coordinates of sampling locations were determined in the field using the GNSS and were transformed from WGS84 coordinate system into the local Gauss-Krüger metric coordinate system. Location of the gauging station Podhom was obtained from the Environment Agency of the Republic of Slovenia (Internet 2). As a base map, we used a high-resolution (1 × 1 m) digital elevation model (DEM) of Slovenia obtained by laser scanning (lidar) in 2014–2015 and changed the geological map to being slightly transparent, to preserve the visualization of relief surface.

Results and discussion

The results for temperature, pH, electrical conductivity, and dissolved oxygen (DO) are reported in Table 1. Measured and calculated variables (T, pH, EC, DO, m_{TSS}, total alkalinity, log pCO_2, $\delta^{13}C_{DIC}$, $\delta^{13}C_{POC}$) versus time (date) in our study are presented in Supplementary material (SM).

The temperature ranged from 6.6 to 8.6 °C, pH from 7.9 to 8.1, and electrical conductivity from 275 to 318 μS/cm (Table 1, SM Figs. A, B, C). The temperature was the highest in June 2024. pH was higher during autumn months, and lower during spring. The highest electrical conductivity was in October 2024, while the lowest during spring. The stream water was oversaturated with oxygen (Table 1, SM Fig. D), as the saturation point is reached at 8.3 mg/l at 25 °C (Atkins, 1994). DO was the lowest in autumn month, and the highest in spring 2024 (SM Fig. D). Electrical conductivity was typical for pristine carbonate catchment at their source (Kanduč et al., 2007a). Further, we compared electrical conductivity measured in the stream with the measurements in the Radovna River during the other studies (Torkar & Brenčič, 2015; Torkar et al., 2016). Seasonal measurements conducted in February 2006, February 2008, September 2008, and March 2009 revealed lower electrical conductivities in the Radovna River, ranging from 213 to 287 μS/cm, along the entire stretch from its source to its confluence with the Sava River (Torkar & Brenčič, 2015). In a later study by (Torkar et al., 2016) electrical conductivity showed a wider range due to more intensive sampling, spanning the period from May 2005 to December 2007, with values ranging from 222 to 325 μS/cm.

Daily precipitation (P_{daily}) ranges from 0-20.6 mm (Internet 1), while daily discharge at Podhom on the River Radovna (Q_{daily}) ranges from 4 to 18.2 m^3/s (Table 1) during the investigated period. The mass of total suspended solids ranged from 0.05 to 0.2 mg/L (Table 1, SM Figure E) on a monthly basis, being higher in September 2023 due to higher discharge and precipitation, and lower in March 2023 when there was no precipitation. In this study, the mass of suspended matter ranged from 0.1 to 0.8 mg/L, which, according to Meybeck (1981), classifies it within the first class. The mass of total suspended matter in the River Sava catchment in Slovenia ranged from 0.5 to 313 mg/L, as measured in late summer 2004 and in spring, 2005 (Kanduč et al., 2007b) placing it in the fourth class according to Meybeck (1981).

Total alkalinity ranges from 2.2 to 2.7 mM being lower in summer months due to lower discharges (Table 1, SM Fig. F).

Log pCO_2 ranged from -3.4 to -2.8, $\delta^{13}C_{DIC}$ from -11.8 to -9.7 ‰, while $\delta^{13}C_{POC}$ from -29.4 to -24.9 ‰, respectively (Table 1, SM Figs. G, H, I).

Table 1. Results of measured variables in the headwater stream recharged by Lipnik springs (July 2023 - May 2024).

Lab ID	**year-month--day**	**P_{daily}* (mm) at Zg. Radovna**	**Q_{daily}* (m^3/s) at Podhom**	**T (°C)**	**pH**	**Electrical conductivity (µS/cm)**	**Dissolved oxygen (mg/L)**	**m_{TSS} (mg/L)**	**Total alkalinity (mM)**	**log pCO_2**	**$\delta^{13}C_{DIC}$ (‰)**	**$\delta^{13}C_{POC}$ (‰)**
23-208	2023-07-20	20.6	4.0	8.6	8.0	297	11.0	0.2	2.5	-2.9	-9.8	-29.4
23-306	2023-08-31	4.6	10	n.d.	8.0	n.d.	n.d.	0.2	2.5	-2.8	-11.8	-26.1
23-352	2023-09-29	4.0	5.4	7.0	7.9	318	11.1	0.8	2.7	-2.8	-11.2	-28.2
23-383	2023-10-24	0.5	18.2	7.2	7.9	300	11.3	0.5	2.2	-2.9	-11.8	-27.1
23-428	2023-11-29	0	5.3	6.6	8.1	308	11.8	0.2	2.2	-3.1	-10.7	-28.2
24-192	2024-03-18	0	7.8	7.7	8.0	300	12.0	0.05	2.3	-2.9	-11.1	-24.9
24-265	2024-05-13	5.1	7.0	8.5	7.9	275	11.0	0.3	2.6	-3.4	-9.7	-26.3

n.d. – not determined, pCO_2 – partial pressure of CO_2, $\delta^{13}C_{DIC}$ – isotopic composition of dissolved inorganic carbon, $\delta^{13}C_{POC}$ – isotopic composition of particulate organic carbon, m_{TSS} – mass of total suspended solids *data provided by EARS (Environmental Agency of the Republic of Slovenia)

Log pCO_2 values indicate that during all sampling period, the CO_2 was releasing to the atmosphere (Figure 3, SM Fig. G). Calculated log pCO_2 is one to four times higher than recent atmospheric value of pCO_2 (Lan et al., 2024). pH is approximately 8, which is typical for investigated stream and also for waters draining carbonate rocks. When waters interact with these rocks, a buffering reaction occurs, typically leading to a neutral to slightly alkaline pH. HCO_3^- acts as a buffer and helps maintaining pH in the range of 7 to 8.

Figure 4 shows $\delta^{13}C_{DIC}$ versus total alkalinity. Changes in-stream indicate processes affecting $\delta^{13}C_{DIC}$, e.g. respiration of organic matter, carbonate mineral dissolution, and equilibration with atmospheric CO_2 (Barth et al., 2003). Therefore, the $\delta^{13}C_{DIC}$ of the headwater stream is controlled by bedrock lithology, the degradation of organic matter (vegetation), and equilibration with atmospheric CO_2. The headwater stream is surrounded by narrow hill slopes covered with mixed forest composed of C_3 plants (Kanduč et al., 2012) growing over carbonate bedrock. Runoff events flush vegetation and soil material with different $\delta^{13}C$ values into the stream.

The prevailing forest communities in the Sava River watershed are various types of European beech (*Fagus sylvatica* L.) forests. At higher altitudes (900–1500 m), European beech is associated with Norway spruce (*Picea abies* (L.) Karst.), silver fir (*Abies alba* P. Mill.), and European larch (*Larix decidua* P. Mill.) (Kanduč et al., 2007b). *Fagus sylvatica* has a $\delta^{13}C$ value of –34.8 ‰ (Kanduč et al., 2007b). The leaves and needles of *Picea abies* and *Fagus sylvatica* have $\delta^{13}C$ values of –30.4 ‰ (Kanduč et al., 2025).

Measured $\delta^{13}C_{POC}$ in the headwater stream has an average value of –27.1 ‰. We measured an average $\delta^{13}C_{soil}$ of -26.2 ‰ for the Sava River Basin (Kanduč et al., 2007b). The carbonate bedrock in the catchment area has a $\delta^{13}C$ value of 3.3‰ (Kanduč et al., 2012).

An average $\delta^{13}C_{POC}$ of –27.1 ‰ was assumed to calculate the isotopic composition of DIC derived from in-stream respiration. Open system equilibration of DIC with CO_2 enriches DIC in ^{13}C by about 9 ‰ (Mook et al., 1974), thus yielding the estimate of –18.1 ‰ shown in Figure 4 (line 4). Nonequilibrium dissolution of carbonates with one part of DIC originating from soil CO_2 (–27.1 ‰), and the other from carbonates with an average $\delta^{13}C_{Ca}$ of 3.3 ‰, produces an intermediate $\delta^{13}C_{DIC}$ value of –11.9 ‰ (line 3 in Fig. 4). Given the isotopic composition of atmospheric CO_2 (–7.8 ‰ Levin et al., 1987) and the equilibrium fractionation with DIC of +9 ‰, DIC in equilibrium with the atmosphere should have a $\delta^{13}C_{DIC}$ of about -1.2 ‰ (line 2 in Fig. 4). Dissolution of carbonates provides 1 ‰ enrichment with ^{12}C isotope (Romanek et al., 1992) and gives a value of 2.3 ‰ (line 1, Fig. 4). Stream samples (Fig. 4) fall around fractionation line (3), which presents nonequilibrium carbonate dissolution by carbonic acid produced from soil zone with a $\delta^{13}C_{CO2}$ of -27.1 ‰.

By solving equations (2) and (3), we calculated F_{DICorg} (molC/day) and $F_{DICcarb}$ (molC/day) (Table 2), and subsequently determined the contribution of biogeochemical processes in the stream. The dominant biogeochemical process in the stream is the dissolution of carbonates (from 50.3 to 57.3 %), followed by the degradation of organic matter (from 42.8 to 49.7 %), while the smallest contribution comes from equilibration with atmospheric CO_2 (from 0.01 to 0.11 %) (Table 2). Other investigated rivers in Slovenia with diverse flow regimes—such as the Sava River (Alpine rain-snow regime), Krka River (Dinaric-Alpine rain-snow regime) (Zavadlav et al., 2013), Kamniška Bistrica River (Alpine high-mountain nival-pluvial regime), and Idrijca River (nival-pluvial karstic flow regime) (Kanduč et al., 2017)—also exhibit similar contributions of biogeochemical processes. Among these, carbonate dissolution is the most dominant, followed by organic matter degradation, while atmospheric exchange represents the least significant process. The lowest $\delta^{13}C_{DIC}$ with value of -11.8 ‰ is observed in August and October 2023 (SM Fig. H) due to higher discharge condition in stream, while the lowest (-9.7 ‰) in May 2024 meaning that nonequilibrium dissolution of carbonates with one part of DIC originating from soil CO_2 and the other from carbonates is dominant. Completely different $\delta^{13}C_{DIC}$ was found in McMurdo Cry Valley streams. The $\delta^{13}C$ values from McMurdo Dry Valley (Lyons et al., 2013) streams span a range of greater than 14 ‰, from -9.4 ‰ to +5.1 ‰, with the majority of samples falling between -3 ‰ and +2 ‰, suggesting that inorganic in source. Because there are no vascular plants on this landscape and no groundwater input to these streams, atmospheric exchange is the dominant control on $\delta^{13}C_{DIC}$. For example, the latest study indicates that $\delta^{13}C_{DIC}$ ranges from -13.3 to -8.0 ‰ in silicate River Oplotnica catchment, meaning that only equilibration of CO_2 and degradation of organic matter influence $\delta^{13}C_{DIC}$ values (Kanduč et al., 2025), which suggests that biogeochemical processes within the specific catchment area have an effect on the $\delta^{13}C_{DIC}$ values. The $\delta^{13}C_{DIC}$ values investigated in the study of the Varaždin alluvial aquifer, which is characterized by overfertilization (Karlović et al., 2022), are compared to $\delta^{13}C_{DIC}$ values found in a headwater stream. The $\delta^{13}C_{DIC}$ values varied seasonally from −13.6 ‰ to −0.5 ‰ in surface water samples and from −14.5 ‰ to −10.7 ‰ in groundwater samples. The $\delta^{13}C_{DIC}$ values in both surface water and groundwater from the Varaždin aquifer span a wider range than those in the headwater stream ($\delta^{13}C_{DIC}$ from −11.8 ‰ to −9.7 ‰), due to different biogeochemical processes influencing the $\delta^{13}C_{DIC}$ signature. In the Varaždin aquifer study, the highest oscillations of $\delta^{13}C_{DIC}$ and other tracers (DIC, DOC) were observed in the gravel pit. More negative $\delta^{13}C_{DIC}$ values were detected during the warmer months, attributed to increased degradation of organic matter leached from terrestrial sources. In shallow groundwater, more negative $\delta^{13}C_{DIC}$ values were measured compared to deeper groundwater.

We find no correlation between $\delta^{13}C_{POC}$ and $\delta^{13}C_{DIC}$ (Fig. 5). More positive $\delta^{13}C_{POC}$ values are associated with highly degradable soil matter, while plant debris exhibits more negative $\delta^{13}C_{POC}$ values (Fig. 5). Suspended organic matter in rivers is mostly derived from soil and plant material. Therefore, the isotopic composition of suspended organic matter ($\delta^{13}C_{POC}$) in rivers has been used to determine the contribution of terrestrial vegetation and soil matter in the river ecosystems (Ittekot, 1988). The $\delta^{13}C$ values of C3 plants range from -32.0 to -20.0 ‰, while C4 plants range from -15 ‰ to -9.0 ‰ (Deines, 1980). C3 plants in the Sava River catchment in Slovenia have $\delta^{13}C$ values ranging from -34.8 ‰ (*Fagus sylvatica*) to -29.2 ‰ (*Clematis vitalba*) (Kanduč et al., 2007b). The $\delta^{13}C_{POC}$ values in the Lipnik stream range more widely, from -29.4 to -24.9 ‰ (SM Fig. 1), while for the Sava River (2004-2005), $\delta^{13}C_{POC}$ values range from -29.2 to -25.1 ‰ (Kanduč et al., 2007b). The $\delta^{13}C_{POC}$ values (Table 1, Fig. 5) in our study indicate that the particulate organic matter is composed of degraded soil material derived from plant

Table 2. Results of mass balance calculation for evaluation of biogeochemical processes based on total alkalinity and isotopic composition of dissolved inorganic carbon ($\delta^{13}C_{DIC}$) at three different discharge conditions (July 2023, October 2023, May 2024).

year-month-day	**F_{DICex} [molC/day]**	**F_{DICorg} [molC/day]**	**F_{DICCa} [molC/day]**	**F_{DICex} [%]**	**F_{DICorg} [%]**	**F_{DICCa} [%]**
2023-07-20	$9.5 \cdot 10^2$	$3.7 \cdot 10^5$	$4.8 \cdot 10^5$	0.11	43.1	56.8
2023-10-24	$1.1 \cdot 10^3$	$1.7 \cdot 10^6$	$1.7 \cdot 10^6$	0.03	49.7	50.3
2024-05-^{13}	$9.2 \cdot 10^1$	$6.8 \cdot 10^5$	$9.1 \cdot 10^5$	0.01	42.8	57.2
Range	$9.2 \cdot 10^1$-$1.1 \cdot 10^3$	$3.7 \cdot 10^5$-$1.7 \cdot 10^6$	$4.8 \cdot 10^5$-$1.7 \cdot 10^6$	0.01-0.11	42.8-49.7	50.3-57.2
Average	$7.2 \cdot 10^2$	$9.2 \cdot 10^5$	$1.0 \cdot 10^6$	0.05	45.2	54.8

F_{DIC} – the mass flux of dissolved inorganic carbon, ex – equilibration of CO_2 between atmosphere and water, ca – dissolution of carbonates, org – degradation of organic matter.

litter leached from slopes (Fig. 6). More negative δ^{13}C values suggest less degraded organic matter, while more positive values indicate more degraded organic matter. A schematic overview of carbon cycling dynamics with δ^{13}C in different carbon storage compartments in a headwater stream is presented in Figure 6.

No significant correlations were found between the measured parameters at $p<0.05$, except strong negative correlations between electrical conductivity and water temperature (-0.91), which are both connected with discharge and residence time of water in the aquifer among other, m_{TSS} and pH (-0.84), and $\delta^{13}C_{DIC}$ versus log pCO_2 (-0.77).

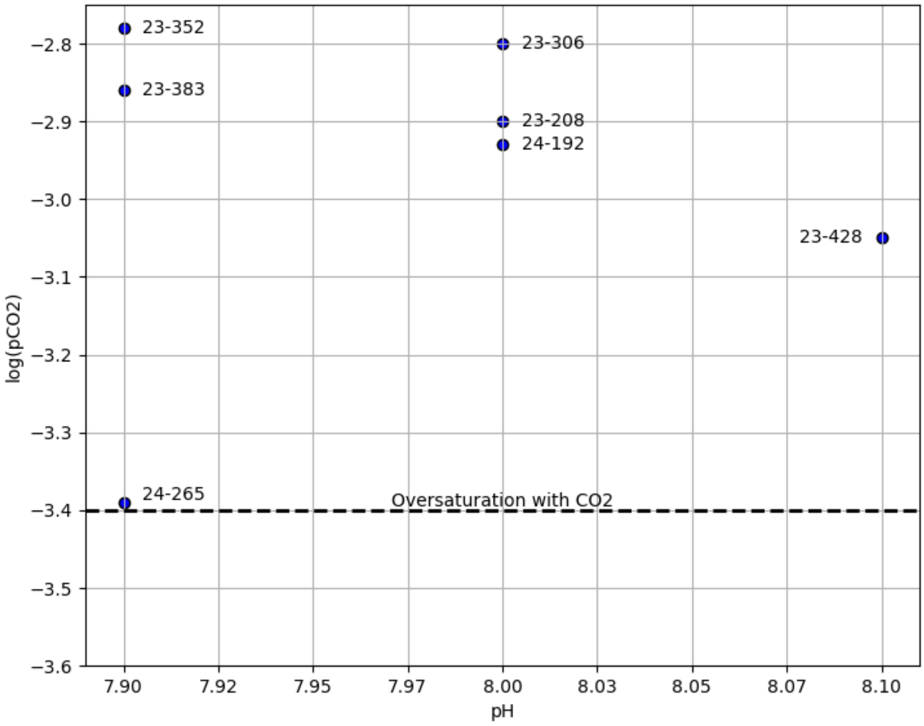

Fig. 3. log pCO_2 versus pH.

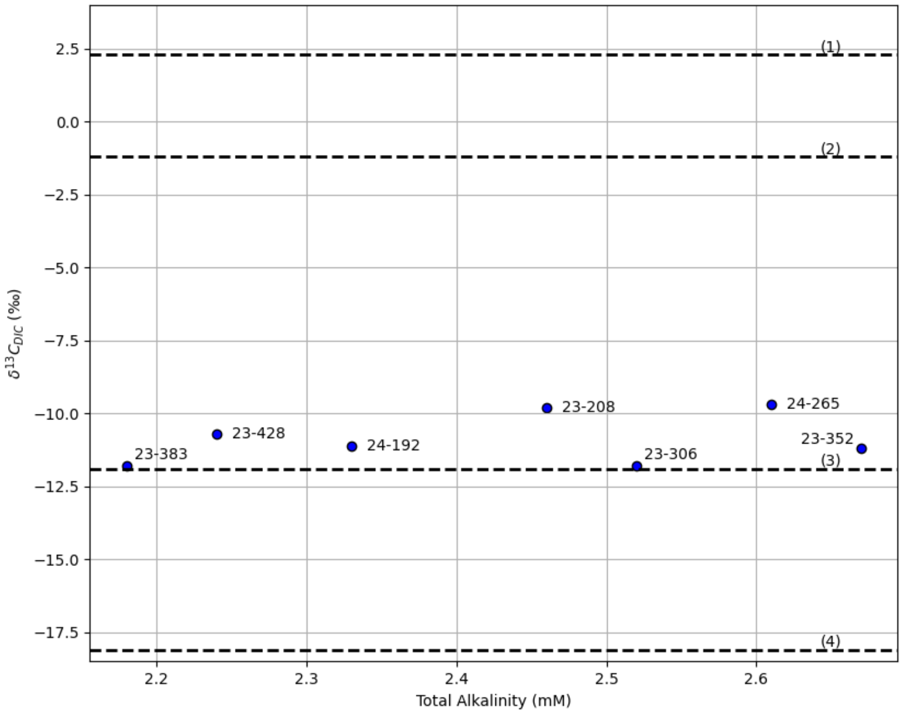

Fig. 4. $\delta^{13}C_{DIC}$ versus total alkalinity; 1 – equilibration with atmospheric CO_2 with value of 1.2 ‰, 2 – dissolution of carbonate with average $\delta^{13}C_{CaCO3}$ of 3.3 ‰, 3 – nonequilibrium carbonate dissolution by carbonic acid produced from soil zone with a $\delta^{13}C_{CO2}$ of -27.1 ‰, 4 – open system equilibration of DIC with soil CO_2 originating from degradation of organic matter with a $\delta^{13}C_{CO2}$ of -27.1 ‰.

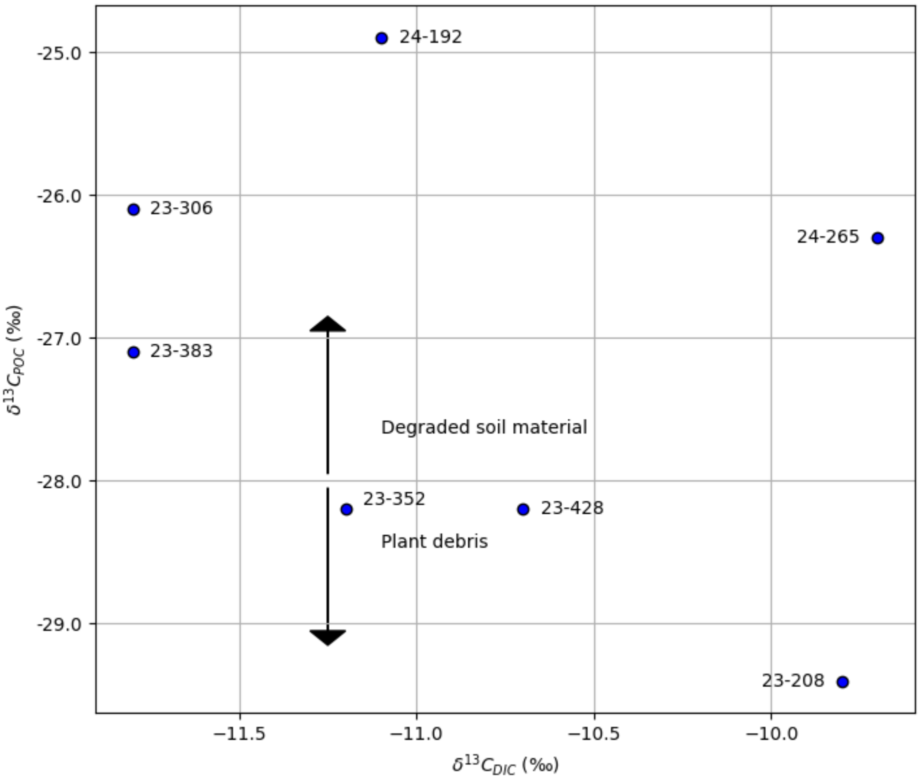

Fig. 5. $\delta^{13}C_{POC}$ versus $\delta^{13}C_{DIC}$.

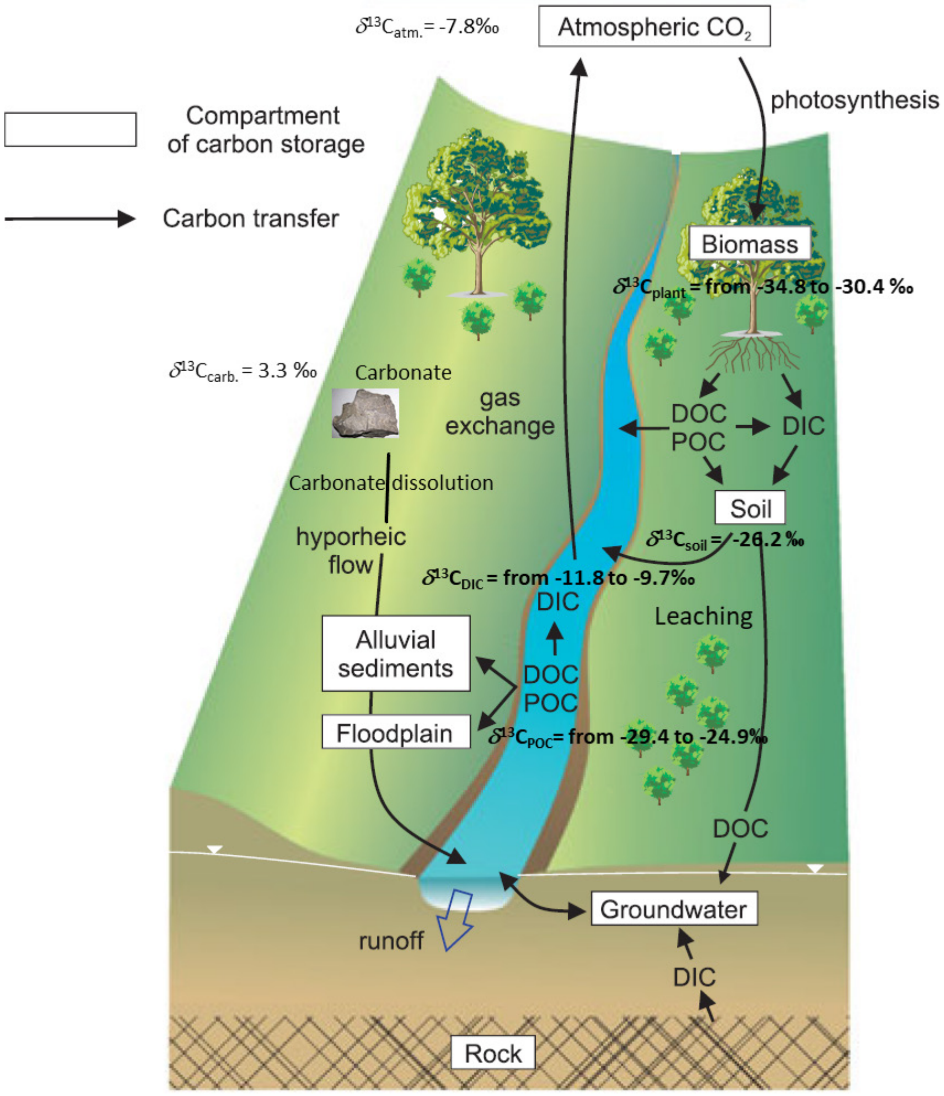

Fig. 6. Schematic overview of carbon cycling dynamics with $\delta^{13}C$ in a headwater stream (adapted from Marx et al., 2017 , reproduced with permission). $\delta^{13}C_{plant}$ – isotopic composition of carbon in plant litter (data from Kanduč et al., 2007b), $\delta^{13}C_{soil}$ – isotopic composition of carbon in soil (data from Kanduč et al., 2007b), $\delta^{13}C_{POC}$ – isotopic composition of carbon in particulate organic matter, $\delta^{13}C_{DIC}$ – isotopic composition of carbon in dissolved inorganic carbon, $\delta^{13}C_{carb.}$ – isotopic composition of carbon in carbonate (data from Kanduč et al., 2012), $\delta^{13}C_{atm.}$ – isotopic composition of carbon in atmospheric CO_2 (data from Levin et al., 1987).

Conclusion

This study confirmed the role of headwater streams as important contributors of CO_2 to the atmosphere, as well as the importance of groundwater recharge and soil leaching for the geochemical processes in such streams. Total alkalinity ranged from 2.2 to 2.7 mM, which is typical for carbonate pristine catchment. The sampled stream water was supersaturated with CO_2 in all months, and represents a source of CO_2 into the atmosphere. Seasonal variations in the stable isotope composition of carbon ($\delta^{13}C_{DIC}$) were due to differences in discharge conditions, being lower during high discharge conditions due to dilution with precipitation and higher during low discharge conditions.

The biogeochemical processes affecting total alkalinity and $\delta^{13}C_{DIC}$ (ranging from -11.8 to -9.7 ‰) indicate that carbonate dissolution has the most significant impact on $\delta^{13}C_{DIC}$ in the carbonate catchment, contributing 50.3–57.0 %, followed by the degradation of organic matter, contributing 42.8–49.7 %. Equilibration with atmospheric CO_2 has a minimal impact (ranging from 0.01 % to 0.11 % in our study) under all three-discharge conditions, as the water does not stagnate and does not reach equilibrium with atmospheric CO_2.

Both isotopic compositions ($\delta^{13}C_{DIC}$ and $\delta^{13}C_{POC}$) are considered powerful tools for tracing biogeochemical cycles in freshwater systems. $\delta^{13}C_{DIC}$ is particularly valuable for investigating instream biogeochemical processes (e.g. degradation of organic matter, dissolution of carbonates, and equilibration with atmospheric CO_2).

Acknowledgements

We thank the ARIS research programme P1-0143, P1-0255, P1-0195 for funding, Mr. Stojan Žigon who performed stable isotopic analyses and Mr. Patrik Kušter for creation of scatter plots in Python. The research was conducted in the area of Triglav National Park with their permission and the consent of the landowners.

Author contribution

Tjaša Kanduč, Nataša Mori contributed to conceptualization. Tjaša Kanduč, Nataša Mori, Timotej Verbovšek were responsible for methodology, software, formal analysis, investigation, writing, original draft preparation. Review, editing, funding acquisition and supervisions were performed by Tjaša Kanduč, Nataša Mori, Timotej Verbovšek.

References

Atekwana, E.A. & Krishnamurthy, R.V. 1998: Seasonal variations of dissolved inorganic carbon and $\delta^{13}C$ of surface waters: application of a modified gas evaluation technique. Journal of Hydrology, 205: 260–278.

Atkins, P.W. 1994: Physical Chemistry. Oxford University press, Oxford, 5th Edition: 1031 p.

Barth, J.A.C., Cronin, A.A., Dunlop, J. & Kalin, R.M. 2003: Influence of carbonates on the riverine carbon cycle in an anthropogenically dominated catchment basin: evidence from major elements and stable carbon isotopes in the Lagan River (N. Ireland). Chemical Geology, 200: 203–216.

Battin, T.J., Kaplan, L.A., Newbold, D., Cheng, X. & Richter, A. 2008: Biological and geochemical controls on organic carbon turnover in streams and rivers. Nature Geoscience, 1/11: 665–669. https://doi.org/10.1038/ngeo325

Broecker, W.S. 1974: Chemical oceanography. In: Leeder, MR (ed.): Sedimentology and sedimentary basins. Harcout-Brace-Jovanovich, New York: 592.

Broecker, H.C, Peterman, J. & Siems, W. 1978: The influence of wind on CO_2–exchange in a wind–wave tunnel, including the efects of monolayers. Journal of Marine Research, 36: 595–610.

Buser, S. & Komac, M. 2002: Geological map of Slovenia 1:250,000. Geologija, 45/2: 335–340. https://doi.org/10.5474/geologija.2002.029

Deines, P. 1980: The isotopic composition of reduced organic carbon. In: Fritz, P. & Fontes J.C. (eds.): Handbook of Environmental isotopic Geochemistry, 329–406.

Doctor, D.H., Kendall, C., Sebestyen, S.D., Shanley, J.B., Ohte, N. & Boyer, E.W. 2008: Carbon isotope fractionation of dissolved inorganic carbon (DIC) due to outgassing of carbon dioxide from a headwater stream. Hydrological Processes, 22/14: 2410–2423. https://doi.org/10.1002/hyp.6833

Evans, M.L., Raymond, P.A. & Bauer, J.E. 2024: Tracing sources of stream DIC using $\delta^{13}C$ and $\delta^{14}C$ isotopes. Environmental Research, 244: 117209. https://doi.org/10.1016/j.envres.2024.117209

Gammons, C.H., Babcock, J.N., Parker, S.R. & Poulson, S.R. 2011: Diel cycling and stable isotopes of dissolved oxygen, dissolved inorganic carbon, and nitrogenous species in a stream receiving treated municipal sewage. Chemical geology, 283: 44–55.

Holley, E.H. 1977: Oxygen transfer at the air–water interface. In: Gibbs, R.J. (ed.): Transport processes in lakes and oceans, Proc. Symp. On Transp. Processes in the Ocean held at the 2nd Nat. Meet Of the AICE, Atlantic City, N. J. Aug. 29.–Sep. 1, 1976, 117–150.

Ittekkot, V. 1988: Global trends in the nature of organic matter in the river suspensions. Nature, 332: 436–438. https://doi.org/10.1038/332436a0

Jähne, B., Heinz, G. & Dietrich, W. 1987: Measurments of the Diffusion Coefficients of Sparingly soluble gases in water. Journal of Geophysical Research, 92: 10767–10776.

Kanduč, T., Szramek, K., Ogrinc, N. & Walter, L.M. 2007a: Origin and cycling of riverine inorganic carbon in the Sava River watershed (Slovenia) inferred from major solutes and stable carbon isotopes. Biogeochemistry, 86: ^{13}7–184.

Kanduč, T., Ogrinc, N. & Mrak, T. 2007b: Characteristics of suspended matter in the River Sava watershed, Slovenia. Isotopes in Environmental and Health Studies, 43/4: 369–385.

Kanduč, T., Mori, N., Kocman, D., Stibilj, V. & Grassa, F. 2012: Hydrogeochemistry of Alpine springs from North Slovenia: insights from stable isotopes. Chemical geology, 300–301: 40–54. https://doi.org/10.1016/j.chemgeo.2012.01.012

Kanduč, T., Kocman, D. & Verbovšek, T. 2017: Biogeochemistry of some selected rivers (Kamniška Bistrica, Idrijca and Sava in Slovenia): insights into river water geochemistry, stable carbon isotopes and weathering material flows. Geologija, 60/1: 9–26. https://doi.org/10.5474/geologija.2017.001

Kanduč, T., Vrabec, M., Verbovšek, T., McIntosh, J., Žlindra, D. & Vilhar, U. 2025: Assesing silicate catchment dynamics of the Oplotnica River (Slovenia) through stable carbon and nitrogen isotopes. Aquatic geochemistry, 31/5: 1–33. https://doi.org/10.1007/s10498-025-09439-w.

Karlović, I., Marković, T., Kanduč, T. & Vreča, P. 2022: Assessment of Seasonal Changes on the Carbon Cycle in the Critical Zone of a Surface Water (SW)-Groundwater (GW) system. Water, 14/21: 3372. https://doi.org/10.3390/w14213372

Kendall, C. & McDonell, J.J. 1998: Isotope tracers in catchment hydrology. Elsevier: 794 p.

Knoll, L.B., Hotchkiss, E.R., Hall, R.O. & Sponseller, R.A. 2024: Groundwater-derived carbon stimulates headwater stream CO2 emissions. Water Research, 259: 120741. https://doi.org/10.1016/j.watres.2024.120741

Lan, X., Tans, P. & Thorning, K.W. 2024: Trends in globally –averaged CO_2 determined from NOAA Global Monitoring Laboratory measurements. Version Tuesday, 05-Nov-2024 13: 17:54 MST. https://doi.org/10.15138/9N0H-ZH07

Levin, I., Kromer, B., Wagenback, D. & Minnich, K.O. 1987: Carbon isotope measurements of atmospheric CO_2 at a coastal station in Antarctica. Tellus, 39B: 89–95.

Lyons, W.B., Leslie, D.L., Harmon, R.S., Neumann, K., Welch K.A., Bisson, K.M. & McKnight, D.M. 20^{13}: The carbon stable isotope biogeochemistry of stream. Taylor Valley Antratctica. Applied geochemistry, 32: 26–36.

Marx, A., Dusek, J., Jankovec, J., Sanda, M. Vogel, T., van Geldern, R., Hartmann, J. & Barth, J.A.C. 2017: A Review of CO_2 and Associated Carbon Dynamics in Headwater Streams: A Global Perspective. Reviews of Geophysics, 55/2: 560–585. https://doi.org/10.1002/2016RG000547

Meybeck, M. 1981: River transport of organic carbon to the ocean. In Flux of Organic Carbon to the Oceans, G.E. Likens, F.T. Mackenzie, Richey J.R., Seddell K.K., Turekian K.K. (eds.): U.S. D.O.E. CONF-8009140, Nat. Tech. Ing. Serr. Springfield: 219–269.

Mori, N., Kanduč, T., Opalički, M. & Brancelj, A. 2015: Groundwater drift as a tracer for identifying sources of spring discharge. Groundwater, 53: 123–132. https://doi.org/10.1111/gwat.12314

Mori, N. & Brancelj, A. 20^{13}: Differences in aquatic microcrustacean assemblages between temporary and perennial springs of an alpine karstic aquifer. International journal of speleology, 42/3: 257–266. https://doi.org/10.5038/1827-806X.42.3.9

Mook, W.G., Bommerson, J.C. & Staverman, W.H. 1974: Carbon isotope fractionation between dissolved bicarbonate and gaseous carbon dioxide. Earth Planetary Science Letters, 22: 169–176.

Opalički, M. 2015: Patterns in invertebrate drift from an alpine karst aquifer over a one year period = Dinamika plavljenja vodnih nevretenčarjev iz alpskega kraškega vodonosnika v obdobju enega leta. Acta Carsologica, 44/2: 265–278.

Raymond, P.A., Hartmann, J., Lauerwald, R., Sobek, S., McDonald, C., Hoover, M., Butman, D., Striegl, R., Mayorga, M., Humborg, C., Kartelainen, P., Dürr, H., Meybeck, M., Ciais, P. &

Guth, P. 2013: Global carbon dioxide emissions from inland waters. Nature, 503: 355–359.

Richardson, J.S. 2019: Headwater streams in book: Reference Module in Earth System and Environmental Sciences, Elsevier. https://doi.org/10.1016/B978-0-12-409548-9.11957-8

Romanek, C.S., Grossman, E.L. & Morse, J.W. 1992: Carbon isotopic fractionation in synthetic aragonite and calcite: effects temperature and precipitation rate. Geochimica et Cosmochimica Acta, 46: 419–430.

Serianz, L., Rman, N. & Brenčič, M. 2020: Hydrogeochemical Characterization of a Warm Spring System in a Carbonate Mountain range of the Eastern Julian Alps, Slovenia. Water, 12/5: 1427. https://doi.org/10.3390/w12051427

Torkar, A. & Brenčič, M. 2015: Spatio-temporal distribution of discharges in the Radovna River valley at low water conditions = Prostorska-časovna porazdelitev pretokov v dolini reke Radovne v obdobju nizkih vod. Geologija, 58/1: 47–56. https://doi.org/10.5474/geologija.2015.003

Torkar, A., Brenčič, M. & Vreča, P. 2016: Chemical and isotopic characteristics of groundwater-dominated Radovna River (NW Slovenia). Environmental Earth Science, 75: 1296. https://doi.org/10.1007/s12665-016-6104-5

Utsumi, G.S.A., He, D., Berelson, W.M., Castelao, R.M., Yager, P.L. & Medeiros, P.M. 2025: Influence of the Amazon River on the composition of particulate organic carbon in the western tropical Atlantic Ocean. Geochimica et Cosmochimica Acta, 389: 84–99.

Waldron, S., Lansdown, J.M. & Scott, E.M. 2018: Stable Carbon Isotopes Reveal Soil-Stream DIC Linkages in Headwater Catchments. Journal of Geophysical Research: Biogeosciences, 123/2: 383–399. https://doi.org/10.1002/2017JG004083

Zavadlav S., Kanduč T., McIntosh J.C. & Lojen, S. 2013: Isotopic and chemical constraints on the biogeochemistry of dissolved inorganic carbon and chemical weathering in the karst watershed of Krka River (Slovenia). Aquatic geochemistry, 19/3: 209–230.

Zuliani, T., Kanduč, T., Novak, R. & Vreča, P. 2020: Characterization of bottled waters by multielemental analysis, stable and radiogenic isotopes. Water, 12/9: 2454. http://doi.org/10.3390/w12092454

Electronic sources:

Internet 1: https://meteo.arso.gov.si/uploads/probase/www/hidro/watercycle/text/sl/observation_sites/springs/Lipnik.pdf (15.3.2025).

Internet 2: https://www.arso.gov.si/en/ (7.4.2025).

Supplementary table

Table SM 1: Results of Spearman correlations (significant at p<0.

	P_{daily}	Q_{daily}	Temperature (°C)	pH	Electrical Conductivity (µS/cm)	Dissolved oxygen (mg/L)	m_{TSS}	TA (mM)	log pCO_2	$\delta^{13}C_{DIC}$ (‰)	$\delta^{13}C_{POC}$ (‰)
P_{daily}	1.0	-0.27	0.70	-0.31	-0.609	-0.61	0.34	0.55	0.09	0.34	-0.318
Q_{daily}	-0.27	1.0	0.17	-0.38	-0.28	0.52	0.25	-0.25	0.25	-0.79	0.73
T	0.70	0.17	1.0	0.0	**-0.91***	0.018	-0.11	0.28	0.07	0.04	0.31
pH	-0.31	-0.38	0.0	1.0	-0.019	0.48	**-0.84***	-0.38	-0.27	0.13	-0.06
Cond.	-0.60	-0.28	**-0.91***	-0.019	1.0	-0.05	0.12	-0.14	0.18	-0.1	-0.40
DO	-0.61	0.52	0.018	0.48	-0.05	1.0	-0.39	-0.32	0.23	-0.65	0.61
m_{TSS}	0.34	0.25	-0.107	**-0.84***	0.12	-0.39	1.0	0.42	0.53	-0.32	-0.23
TA	0.55	-0.25	0.28	-0.38	-0.14	-0.32	0.42	1.0	0.25	0.21	-0.02
log pCO_2	0.09	0.25	0.07	-0.27	0.18	0.23	0.53	0.25	1.0	**-0.77***	-0.13
$\delta^{13}C_{DIC}$	0.34	-0.70	0.03	0.13	-0.1	-0.65	-0.32	0.21	**-0.77***	1.0	-0.29
$\delta^{13}C_{POC}$	-0.31	0.73	0.3	-0.05	-0.4	0.61	-0.23	-0.02	-0.12	-0.29	1.0

*Spearman correlations marked as bold are significant at p<0.050, m_{TSS} – mass of total suspended solids, TA – total alkalinity, pCO_2 – partial pressure of CO_2, $\delta^{13}C_{DIC}$ – isotopic composition of dissolved inorganic carbon, $\delta^{13}C_{POC}$ – isotopic composition of particulate organic carbon

Supplementary figures

Figure SM Fig. A: T (°C) versus sampling date

Figure SM Fig. B: pH versus sampling date

Figure SM Fig. C: Electrical conductivity versus sampling date

Figure SM Fig D: DO versus sampling date

Figure SM Fig. E: m_{TSS} versus sampling date

Figure SM Fig. F: TA versus sampling date

Figure SM Fig. G: log pCO_2 versus sampling date

Figure SM Fig. H: $\delta^{13}C_{DIC}$ versus sampling date

Figure SM Fig. I: $\delta^{13}C_{POC}$ versus sampling date

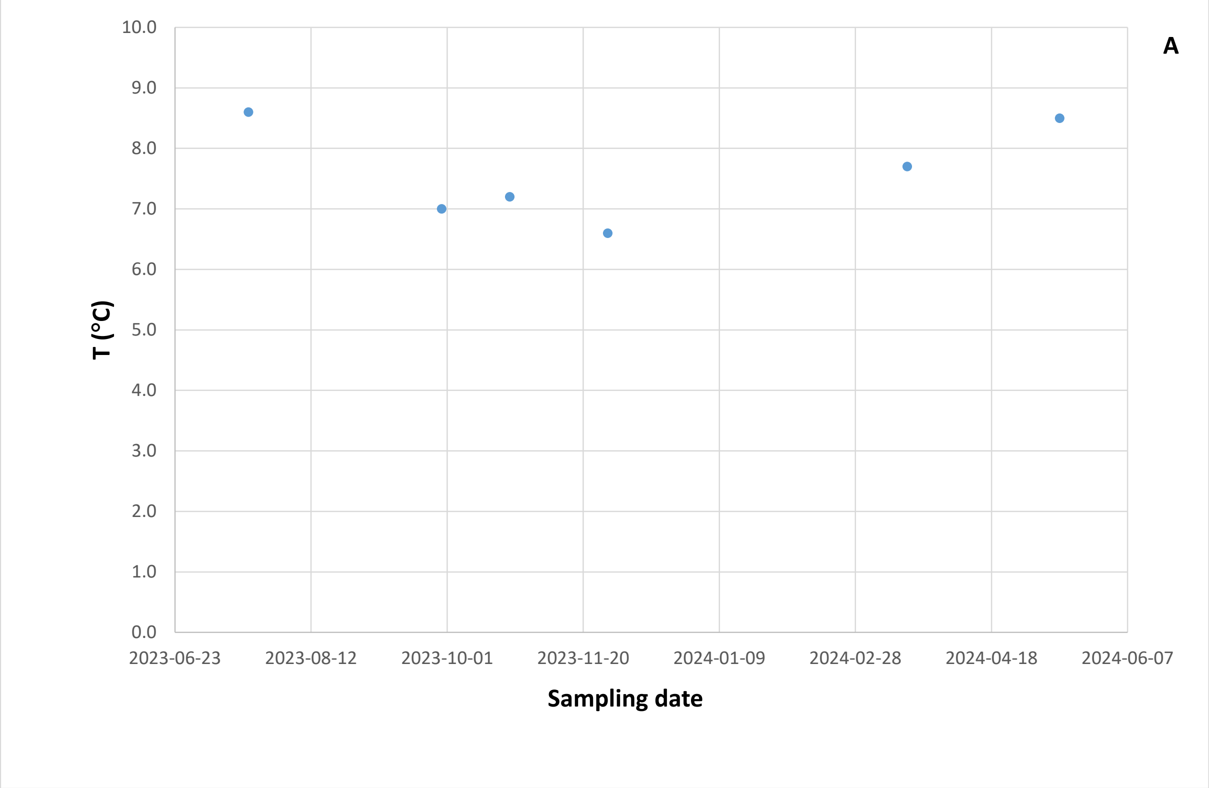

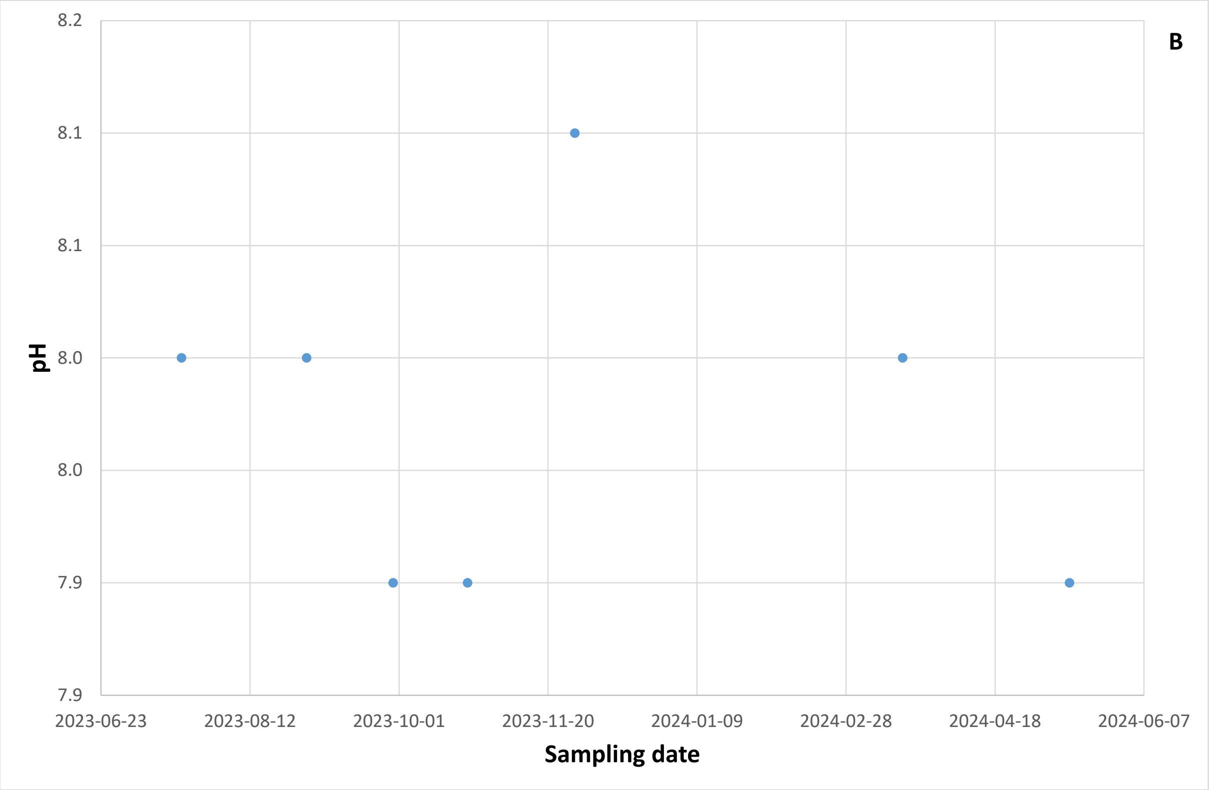
B
pH
8.2
8.1
8.1
8.0
8.0
7.9
7.9
2023-06-23
2023-08-12
2023-10-01
2023-11-20
2024-01-09
2024-02-28
2024-04-18
2024-06-07
Sampling date

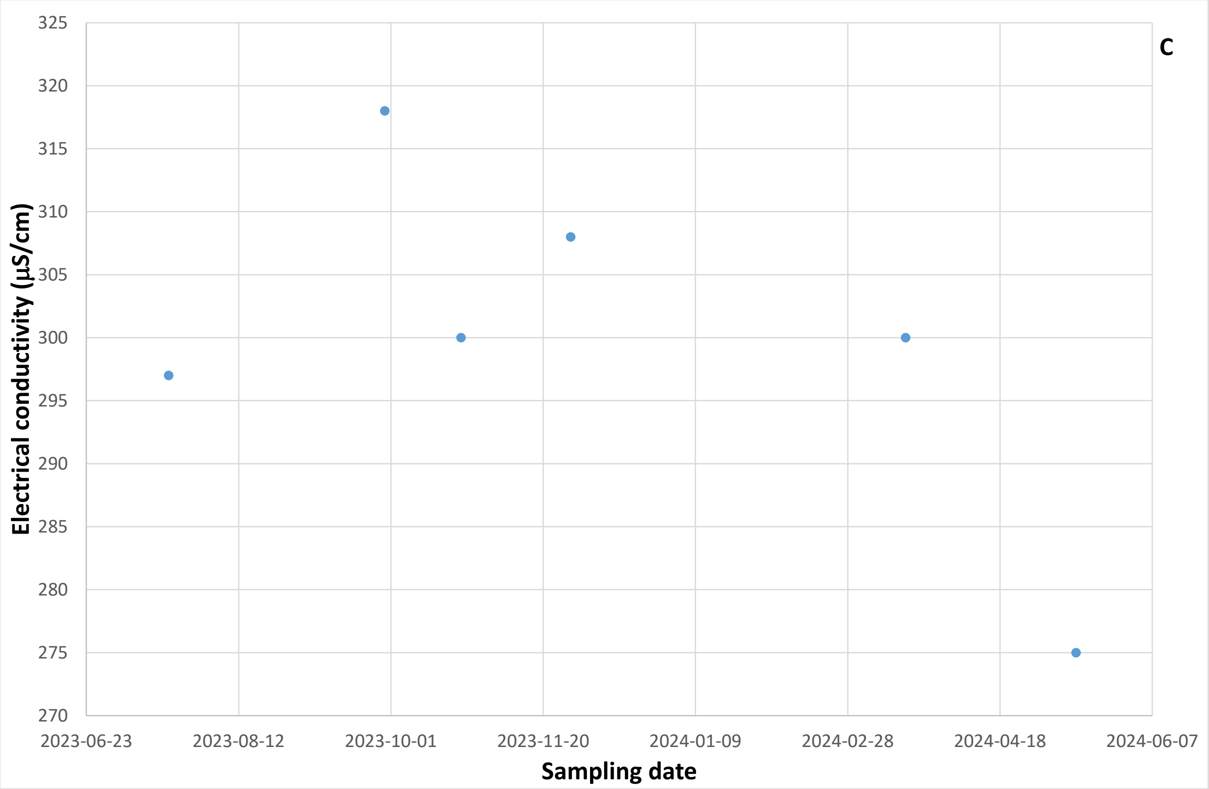
C
Electrical conductivity (µS/cm)
325
320
315
310
305
300
295
290
285
280
275
270
2023-06-23
2023-08-12
2023-10-01
2023-11-20
2024-01-09
2024-02-28
2024-04-18
2024-06-07
Sampling date

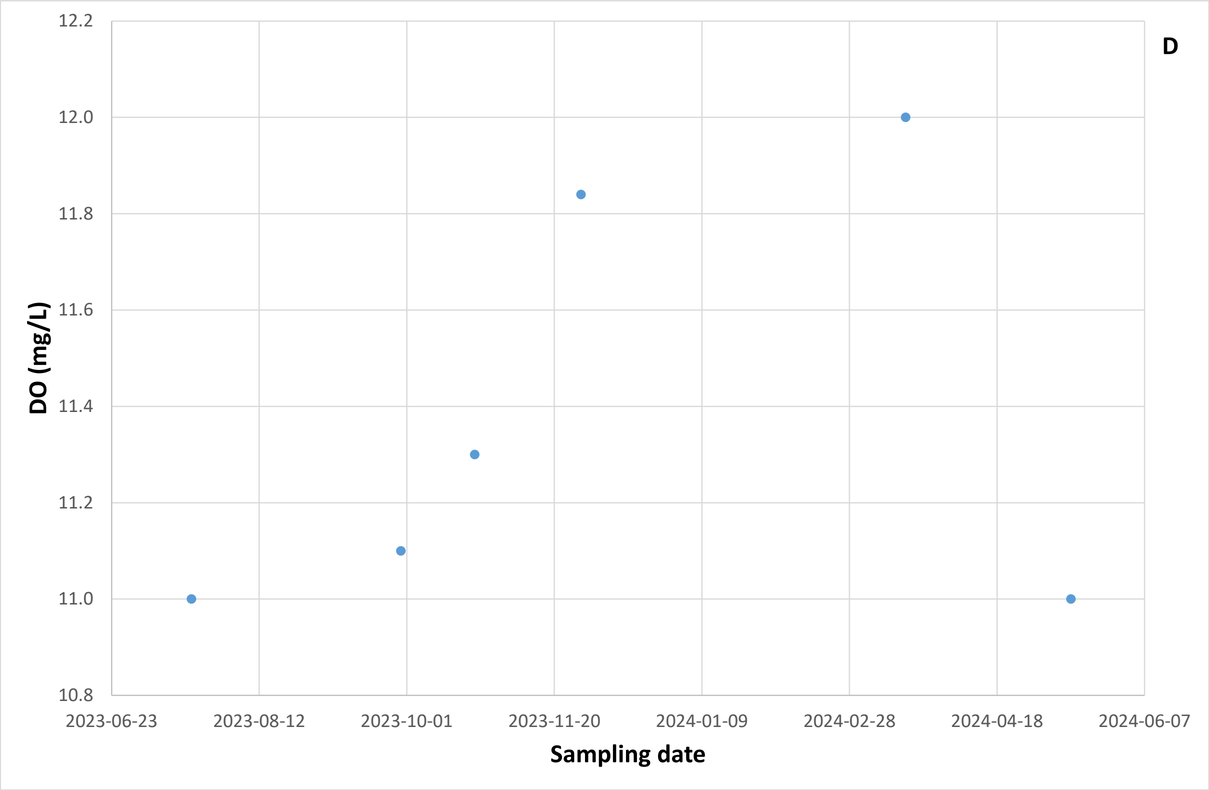
D
12.2
12.0
11.8
11.6
11.4
11.2
11.0
10.8
DO (mg/L)
2023-06-23
2023-08-12
2023-10-01
2023-11-20
2024-01-09
2024-02-28
2024-04-18
2024-06-07
Sampling date

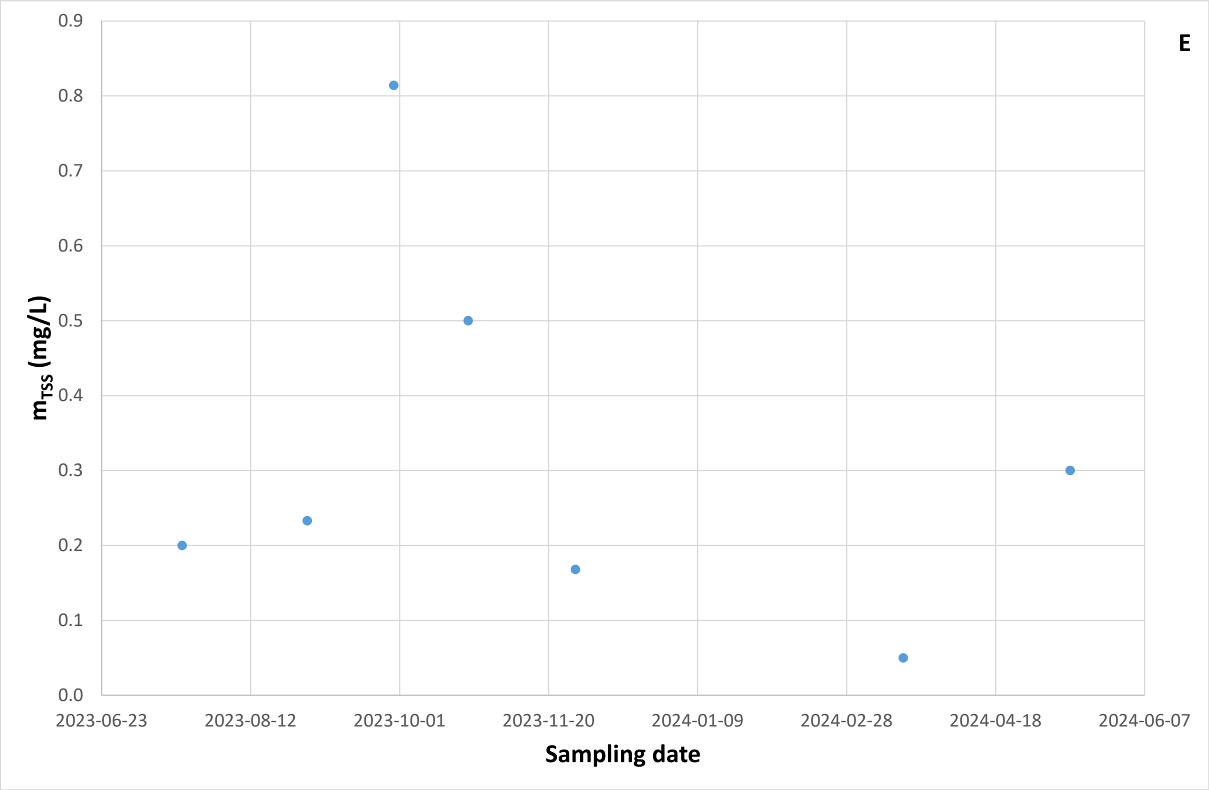
E
0.9
0.8
0.7
0.6
0.5
0.4
0.3
0.2
0.1
0.0
m_{TSS} (mg/L)
2023-06-23
2023-08-12
2023-10-01
2023-11-20
2024-01-09
2024-02-28
2024-04-18
2024-06-07
Sampling date

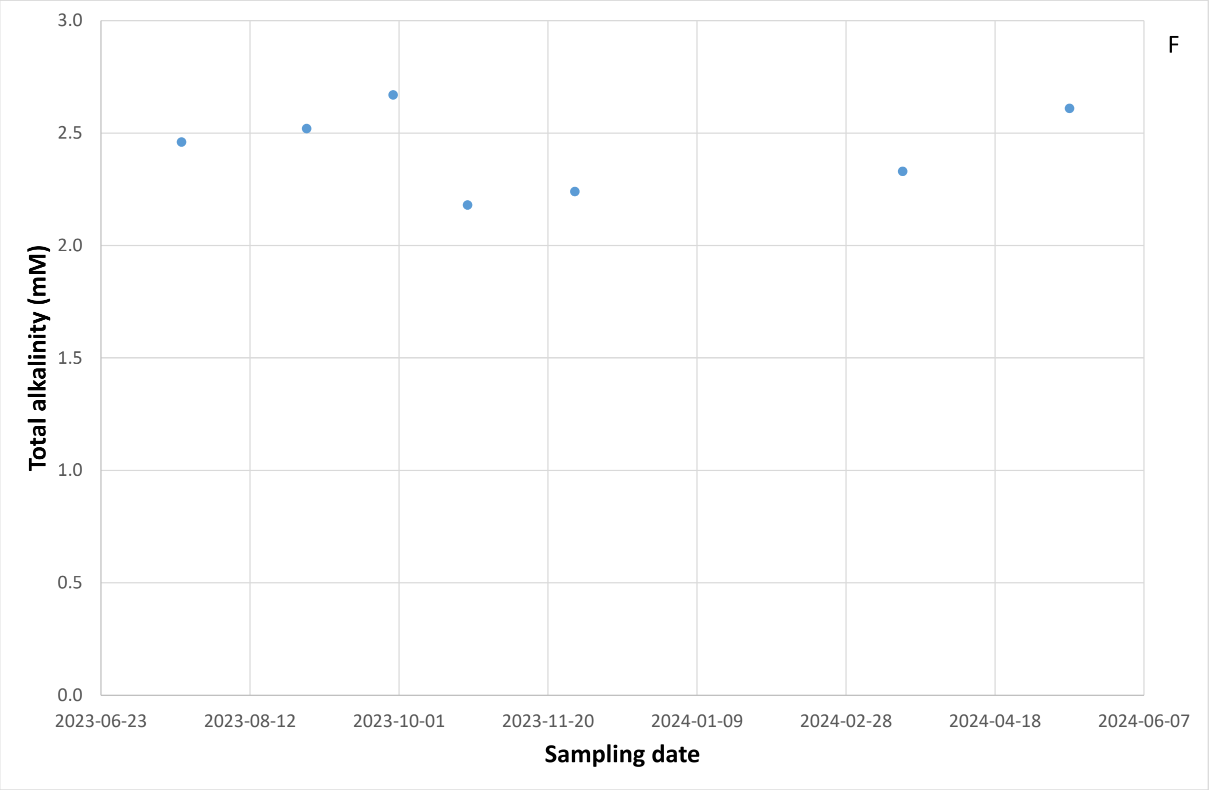
F
Total alkalinity (mM)
3.0
2.5
2.0
1.5
1.0
0.5
0.0
2023-06-23
2023-08-12
2023-10-01
2023-11-20
2024-01-09
2024-02-28
2024-04-18
2024-06-07
Sampling date

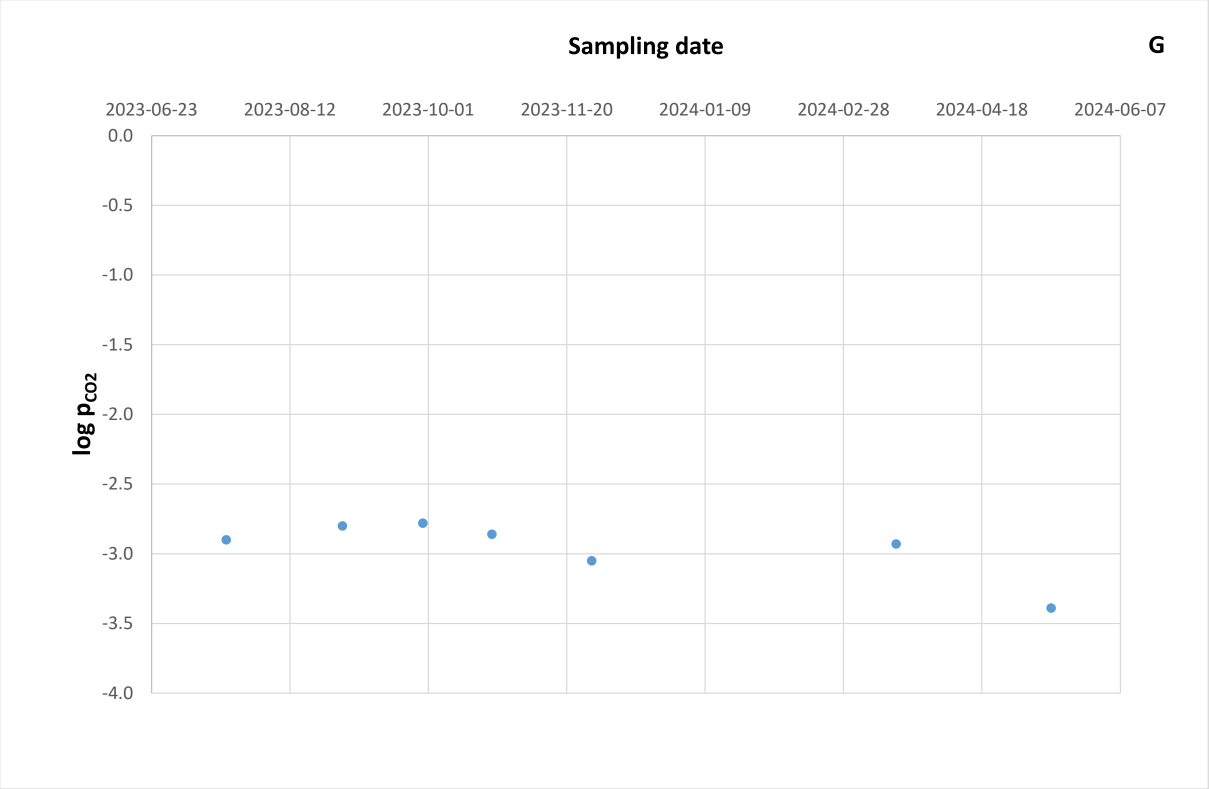
Sampling date
G
2023-06-23
2023-08-12
2023-10-01
2023-11-20
2024-01-09
2024-02-28
2024-04-18
2024-06-07
log p_{CO2}
0.0
-0.5
-1.0
-1.5
-2.0
-2.5
-3.0
-3.5
-4.0

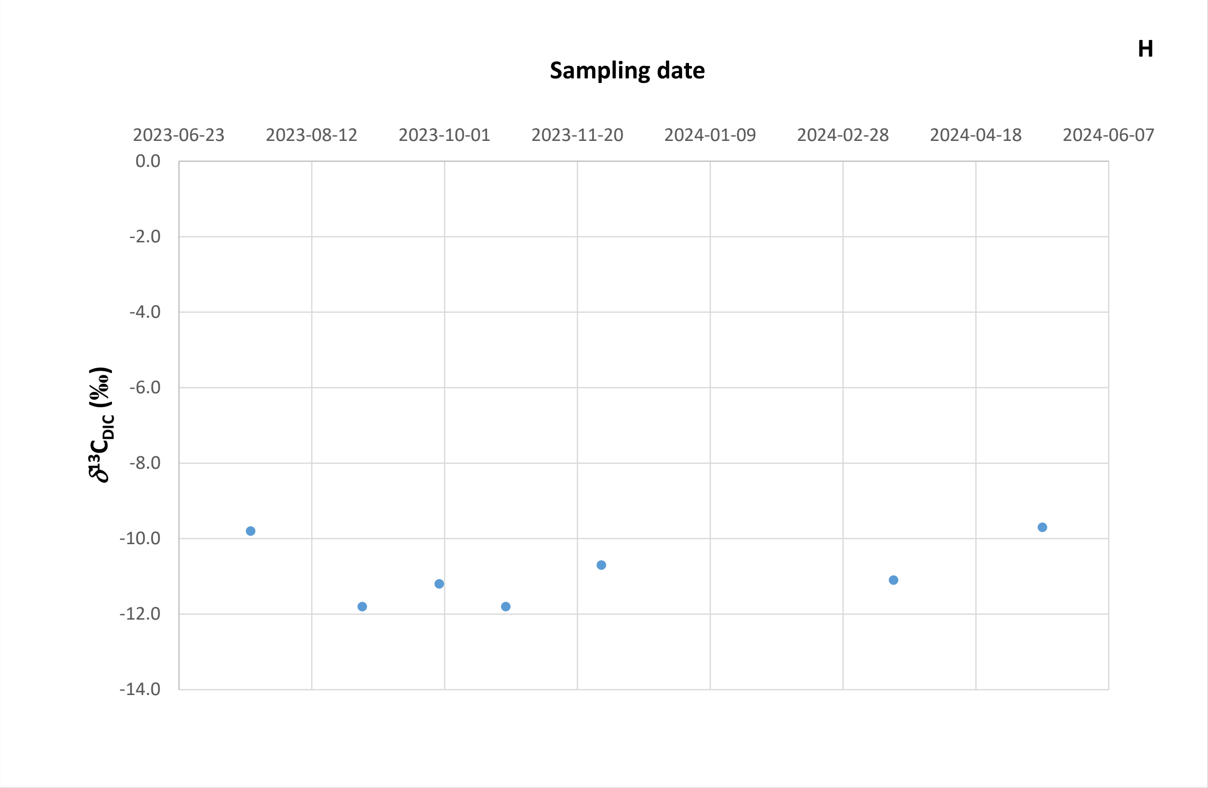
H
Sampling date
2023-06-23
2023-08-12
2023-10-01
2023-11-20
2024-01-09
2024-02-28
2024-04-18
2024-06-07
0.0
-2.0
-4.0
-6.0
-8.0
-10.0
-12.0
-14.0
δ13CDIC (‰)

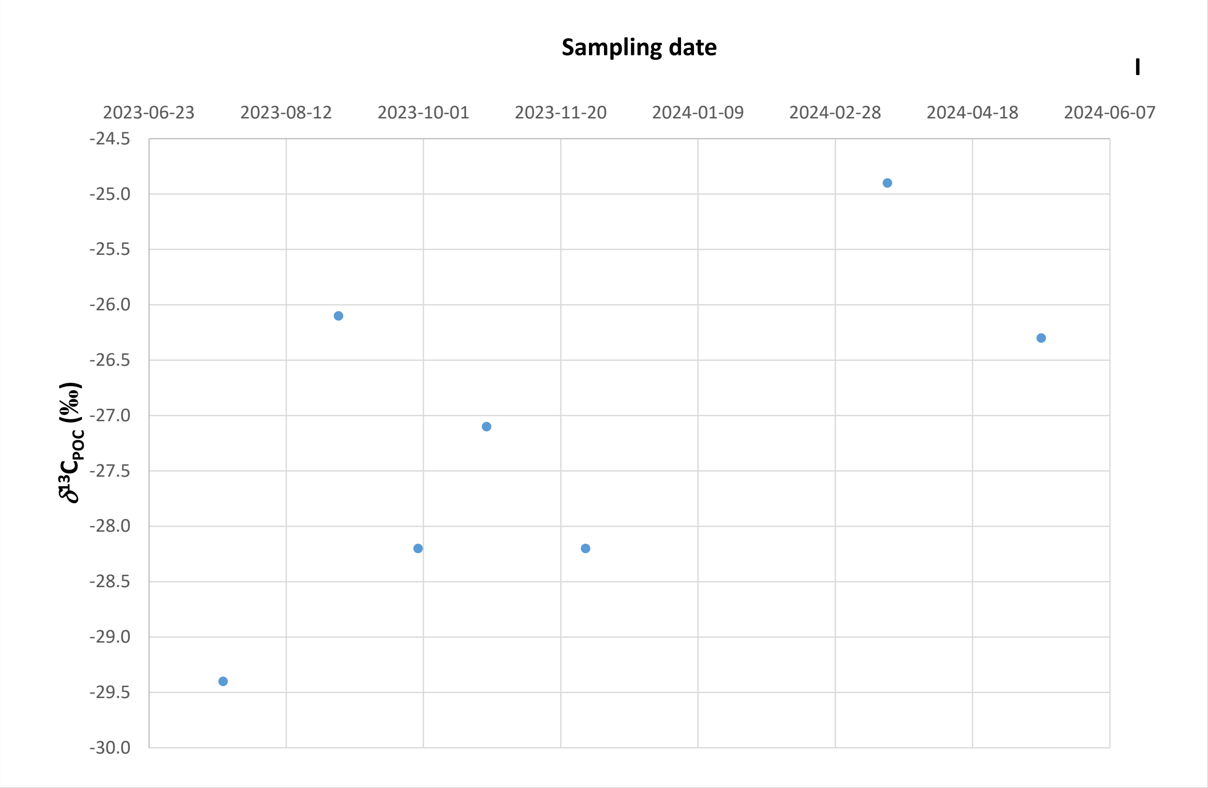
Sampling date
I
2023-06-23
2023-08-12
2023-10-01
2023-11-20
2024-01-09
2024-02-28
2024-04-18
2024-06-07
-24.5
-25.0
-25.5
-26.0
-26.5
-27.0
-27.5
-28.0
-28.5
-29.0
-29.5
-30.0
δ13CPOC (‰)